Al-Khwarizmi Engineering Journal, Vol. 15, No. 4, December, (2019)
P. P. 10- 22

Al-Khwarizmi Engineering Journal

Modeling of Bending Properties of Stainless Steel 304 Sheets Welded by Tungsten Inert Gas Welding Process

Ali Hussein Alwan
Department of Mechanical Engineering/ University of Technology
Email: 20145@uotechnology.edu.iq

(Received 23 May 2019; accepted 25 September 2019)
https://doi.org/10.22153/kej.2019.09.003

Abstract

In this research, the effects of both current and argon gas pressure on the bending properties of welded joints were studied. Using the possible ranges of welding gas pressures and currents, Tungsten inert gas welding (TIG) of stainless steel (304) sheet was used to obtain their influence on the maximum bending force of the (TIG) welded joints. Design of experiment (DOE) 'version 10' was used to determine the design matrix of experiments depending on the used levels of the input factors. Response surface methodology (RSM) technique was used to obtain an empirical mathematical model for the maximum bending force as a function of welding parameters (Current and Argon gas pressure). Also, the analysis of variance (ANOVA) was used to verify the adequacy of the resulted model statistically.

Keywords: *Bending Properties, Numerical Optimization, Stainless Steel (304), TIG Welding, Welding Parameters.*

1. Introduction

Welding is a critical process in the industry since it used to join different materials, especially stainless steels, which are presently used in various structural engineering parts. Welding of tungsten with inert argon gas (TIG) is one of the most important and common industrial processes. The weld efficiency is related to the best selection of main welding parameters, such as welding speed, current, filler material and welding gas pressure. In this section, a review of TIG welding research, welding parameters, the effective welding parameters, type of electrode, covering gases, and welding speed are illustrated.

Anand et al.[1] showed that the TIG welding current 120 A and 309L welding filler produced a higher tensile strength and maximum bending force of the welded joints 310 stainless steel. Tabish et al. [2] concluded that the tensile strength of the stainless steel 304 plate TIG joined specimens was higher than the base material, and the use of low heat input resulted in the best tensile strength and hardness results than other. Navid et al.[3] investigated the heat input in the TIG welding process of 316 stainless steel sheet. It was shown that the increase of current tends to increase the amount of heat input in the welding zone, and this leads to the enlargement of depth and width of the welding pool. Hussein et al. [4] used the (RSM) to develop the mathematical model of TIG welding parameters and the output of the joint strength of 304 stainless sheets. It was shown that 50 A current with 1.6 mm welding filler size and low gas flow rate produced finer weld microstructure without crack, and this leads to high tensile strength of joint. Vikarm and Sharma [5] showed that the lower welding speed range of stainless steel 430 joined by TIG welding produced a higher tensile strength as a result to the formation fine dendritic matrix in the weld zone microstructure. Rohit et al. [6] used the voltage, current, gas flow rate, and welding speed as the input parameters of 304 stainless steel sheets joined by TIG welding. It was

concluded that the neuro-fuzzy inference system for the prediction of tensile properties of welded specimens indicated the accuracy over other the prediction concept (hardness property). Current, welding speed and the flow rate of welding gas were selected by Ravichandran et al. [7] to analyze the TIG welding of duplex stainless steel using signal to noise ratio and (Anova). The analysis showed that the flow rate of welding gas was the most important parameter for the hardness of welded joint and impact strength properties. Aamir et al. [8] concluded that the tensile strength of welded specimens increased with increasing TIG welding pulse current. The increasing of filler feed rate without control of welding current leads to decrease welding strength. Saha and Dhami [9] concluded that the combinations of optimum TIG welding parameters (current, flow rate of gas, speed, and diameter of the electrode) of 304 stainless steel welded joint for tensile properties and hardness only differed in term of welding current. It was found that the optimum value of tensile strength resulted at (180 Amp.), whereas the optimum hardness was at (150 Amp.). The optimization of TIG welding parameters using Taguchi and ANOVA approach of 317 stainless steel plate was investigated by Goyal and Agrawal [10]. It was manifested that the current and welding voltage have a significant effect on the tensile strength more than gas pressure. Jadhav and Wasankar [11] used Taguchi and ANOVA analysis to obtain the optimum values for TIG welding joint hardness and penetration depth of stainless steel 304 that occurred at (150 Amp welding current, and 15 L/min of gas flow rate). Naik et al. [12] found that the welding filler has a minimum effect on the tensile strength and hardness, whereas the welding current has maximum influence on the tensile strength and energy impact of stainless steel 2205 plates joined by TIG welding. Bayrak et al. [13] determined that the decreasing amount of heat input during TIG welding has a positive influence on the mechanical properties of (304 L) stainless steel joint due to the prevented chromium carbide precipitation.

From the above literature, it has been shown that most of the research works focused on the (tensile properties, heat input, corrosion resistance, material of welding filler, and microstructure, etc.) of the joint using TIG welding. Also, some researchers investigated the optimization of welding parameters by using (Taguchi and ANOVA), but a few research considered the use of RSM and analysis of variance (ANOVA) within the design of experiments program. In addition, a few studies considered the modeling of maximum bending force. For this purpose, the aim of the present work is to build a model for the maximum bending force of 304 stainless steel sheets joined by TIG welding and using (DOE) with RSM technique and ANOVA analysis to obtain an empirical equation for the maximum bending force at the optimum welding parameters (current, and gas pressure) by numerical optimization. Confirmation tests will be done at using the optimum input parameters to compare the experimental results with the theoretical ones.

2. Method

2.1. Selection of Material and Specimens Preparation

The sheet of 304 stainless steel alloy was used in the present work which was obtained from the industrial market of (2.0 mm) thickness. The chemical composition of the worked alloy is listed in table (1) according to the ASTM (A240) standard of material [١٤]. The sheets were cut to prepare the required dimensions of welding specimens (200 mm×100 mm) by an electronic cutting machine, and the edges of sheet were ground to ensure that there is no gap between the two mounted specimens, as shown in figure (1).

Table 1,
Chemical composition of stainless steel 304 alloy. [14].

Element	W.t.%	Element	W.t.%
C	0.08	Si	0.750
P	0.0450	Ni	8.0
Mn	2.0	N	0.1
S	0.03	Mo	-
Cr	18		

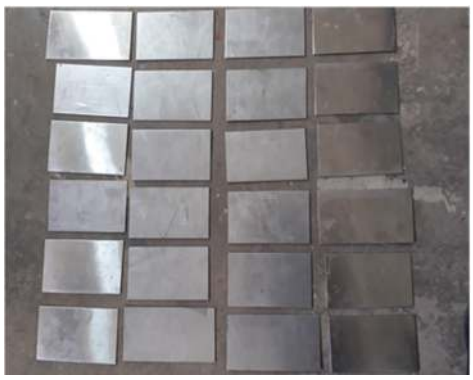

Fig 1. Weld specimen's preparation.

2.2. Procedure of Welding Process

The welding process was done manually by a skilled technician welder in the University of Technology / Workshop Center. To be sure that the two sheets are to be welded in alignment together during the welding process, the sheets were tightly and clamped on the welding board, as explained in figure (2). The TIG 160 welding machine model was used in the present work to accomplish welding of sheets, as shown in figure (3). Table (2) shows the welding machine technical data and welding tools. Through the welding process, the argon gas was used as the inert gas, and the gas flow rate can be manually adjusted by the argon gas organizer, as shown in figure (4). The material of welding filler 304 was used in this work because it is appropriate with the welding specimens material stainless steel 304. The main parameters of welding (current and welding gas flow pressure) were chosen to obtain the best quality of welded joints with a high welding efficiency, i.e., high mechanical and bending properties.

Fig. 2. Workpiece sheets before and after welding process.

Fig. 3. Tig 160 Welding Machine.

Fig. 4. Organizer of Argon Gas.

Table 2,
The welding machine technical data

Power factor.	0.690
Circuit voltage.	65.0 – 80.0Volt
Circuit power.	30Watt
Diameter of Tungsten electrode	1.60 mm
Diameter of welding Filler rod	1.60 mm

2.3 Experimental Design Matrix

The DOE procedure included making mathematical model for the response (max. bending force) in term of input parameters (current and gas pressure), statistical analysis by ANOVA in order to find the model significant or not within 95 percent confidence level, and finding the optimum output (max. bending force) at the optimum input by numerical optimization. Finally, confirmation test is conducted at the optimum conditions for validation purpose in term of the error between the experimental and theoretical result. In this research, DESIGN EXPERT computer programing with the technique of response surface methodology (RSM) was employed to build the matrix of input parameters. The used input parameters in the experimentation processes were selected depending on the previous

experience research. Table (3) lists these factors with two levels. The experimental design was conducted by RSM for two input factors and four responses outputs, with five and four center and axial points, respectively using central composite rotatable design. According to the design of the experimental matrix, thirteen practical runs were performed. Two coded levels (−1 and +1) were used for each parameter, where each code stratifies with a real value tantamount. Thus, welding gas flow pressure and current were the studied input parameters in this work. The input parameters data in terms of real factors are presented in Table (4), which explained the used experimental design matrix.

Table 3,
Levels of Input Parameters used with Coding.

Factors	Units	Low-Level Range (-1)	High-Level Range (+1)
Pressure of Gas Flow	Kg.f/cm^2	13.0	15.0
Welding Current	Amp.	80.0	100.0

2.4 Mechanical Properties Tests

2.4.1 Tensile Test Process.

In the present research, tensile tests were performed in University of Technology/ Laboratories of Mechanical Engineering Department. Tinius Olsen universal testing machine which has a maximum capacity of (5 KN) was used to conduct the tensile test of specimens. A CNC milling machine was used to make the tensile specimens, and the tensile test was restricted according to the American Society for Testing and Materials specifications (ASTM). Figure (5) depicts the geometry design of tensile specimen dimensions for standard (ASEM E8-M) [15]. To evaluate the tensile properties of each welding joint, the average of three specimens was taken in a perpendicular orientation to the welded line and tested at a constant crosshead speed of (1 mm/min) for each case of welding experiment, figure (6). The obtained result of tensile strength, yield stress, and elongation of the welded joint specimens are given in Table (4).

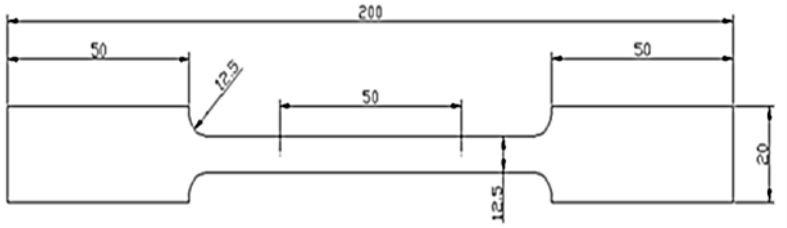

Fig. 5. Rectangular cross-section tensile test specimen according to ASTM E8-M. [1∘] All dimensions are in millimeters.

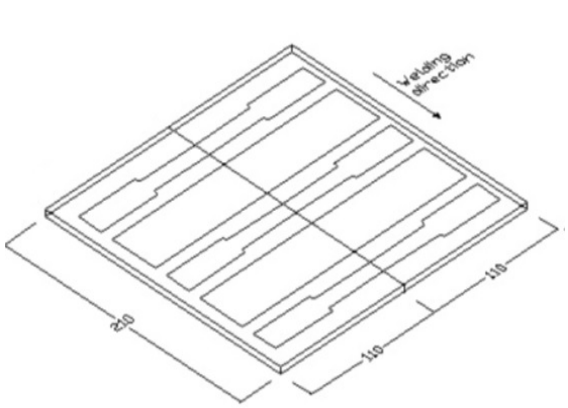

Fig. 6. Tensile test specimens.

2.4.2 Bending Test Process

The bending test was done by Tinius Olsen universal testing machine. The test was achieved at room temperature with a compression speed of (1mm /min). The type of three_ point bending test was used in the present work to evaluate the

maximum bending force. The average of three specimens of each welding case was taken in a perpendicular orientation to the welding line, as revealed in figure (7). The bending test was restricted according to the American Society for Testing and Materials specifications (ASTM E 190) [16].

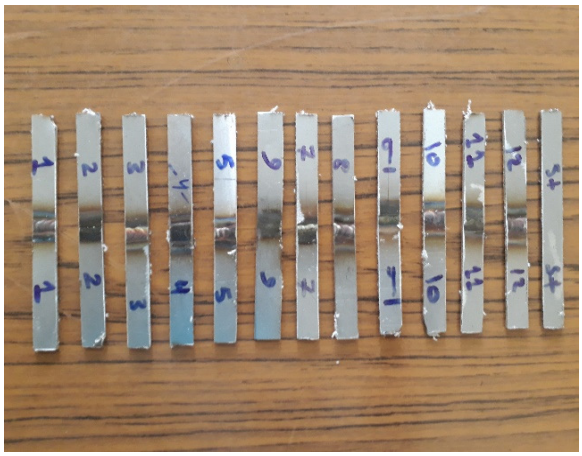

Fig. 7. Bending specimen.

3. Results and Discussion.

3.1 Tensile and bending test results.

After performing the experiments, the welded joints section were examined visually, and the proper portion of the weld surfaces was selected to prepare the tensile and bending specimens. Table (4) shows the results of tensile and bending tests. The tensile strength and maximum bending force of the received base material are 622 MPa and 410 N, respectively. The maximum yield stress was obtained at gas pressure (16 Kgf/cm2), and current (90 Amp.). While the ultimate tensile stress and elongation were obtained at gas pressure (15 Kgf/cm2), and current (80 Amp.).

Table 4,
Design matrix experimental for actual input factors and responses.

Standard No.	Run No.	Gas Pressure (Kgf/cm^2).	Current Ampere.	Yield Stress σ_y (MPa).	Ultimate Tensile Stress σ_u (MPa).	Elongation.	Max. bending Force (N)
1	2	13	80.0	240.0	535.0	28 %	360
2	8	13	100.0	298.0	527.0	44 %	592
3	3	15	80.0	335.0	715.0	44 %	683
4	1	15	100.0	270.0	703.0	20 %	600
5	4	14	70.0	272.0	606.0	38 %	589
6	7	14	110.0	272.0	570.0	27 %	535
7	9	12	90.0	268.0	313.0	40 %	485
8	6	16	90.0	320.0	660.0	31 %	755
9	10	14	90.0	285.0	694.0	31 %	487
10	13	14	90.0	285.0	695.0	35 %	490
11	12	14	90.0	298.0	715.0	32 %	587
12	5	14	90.0	300.0	710.0	34 %	548
13	11	14	90.0	290.0	711.0	35 %	565

In table (4), it can be noted that the highest value of tensile stress occurred at higher gas pressure level and almost at the center of current level (90.0) Amp. This indicates that the gas pressure has a greater influence on the tensile strength than the welding current due to effect of gas protection which was overcame the influence of the heat input caused by current. This result is in agreement with the previous works especially reference (2) which was found that tensile strength of the stainless steel 304 plate TIG joined specimens was higher than the base material, and the use of low heat input resulted the best tensile strength.

3.2 The Maximum Bending Force Model.

The average response obtained for a maximum bending force was used in calculating the model of the response surface per response by using the least-squares method.

For maximum bending force prediction, a diminutive quadratic model in coded terms was analyzed using statistical analysis of variance

(ANOVA) with backward elimination of insignificant coefficients. Table (5) explains the statistical analysis of variance (ANOVA), which created by the software for the remaining terms. The model is significant at 95% confidence. It is observed that the gas pressure (B), the squared term of gas pressure (B^2), and the interaction of current and gas pressure factors (AB) are significant terms with the exception of the current (A), the lack of fit test indicates that a good model was produced. This model explains that only the three terms (B, B^2, and AB) have the highest effect on the maximum bending force.

Table 5,
ANOVA for Response Surface two factors interaction model for Maximum bending force.

Source	Sum of Squares	df	Mean Square	F Value	P-value Prob F	
Model	97360.56	4	24340.14	11.71	0.0020	**significant**
A-Current	140.08	1	140.08	0.067	0.8018	
B-Pressure	63220.08	1	63220.08	30.40	0.0006	
AB	24806.25	1	24806.25	11.93	0.0086	
B^2	9194.14	1	9194.14	4.42	0.0686	
Residual	16634.21	8	2079.28			
Lack of Fit	8533.01	4	2133.25	1.05	0.4805	**not significant**
Pure Error	8101.20	4	2025.30			
Cor Total	1.140E+005	12				
Std. Dev.	45.60			**R-Squared**	0.8541	
Mean	559.69			**Adj. R-Squared**	0.7811	
C.V. %	8.15			**Pred. R-Squared**	0.6063	
PRESS	44880.66			**Adeq. Precision**	12.643	

The final equation of maximum bending force in terms of the actual factors:
Maximum bending force = - 6662.92284 + 110.59167 * Current + 243.54321* Pressure -7.87500 * Current * Pressure + 19.20679 * pressure^2
In term of A & B:
Maximum bending force = - 6662.92284 + 110.59167 * A + 243.54321* B - 7.87500 * AB+ 19.20679 * B^2

For the normal probability plot shown in figure (8) for the maximum bending force data, the residuals that mostly that falling on a straight line implying errors, are normally distributed. And, figure (9) manifests the residuals against the predicted outputs for the results of maximum bending force. Also, it can be observed that no clear patterns or unusual structure exists, indicating that the models are accurate.

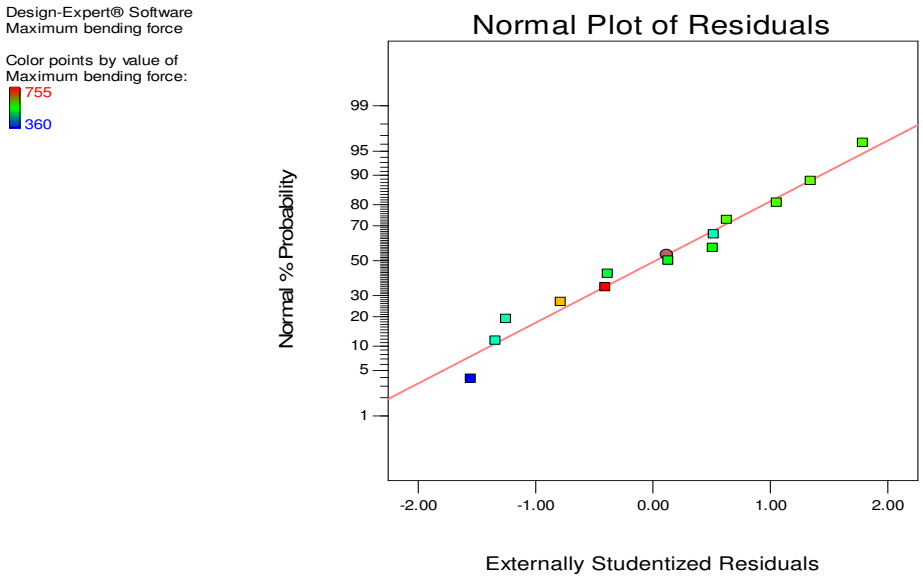

Fig. 8. Normal distribution of maximum bending force data.

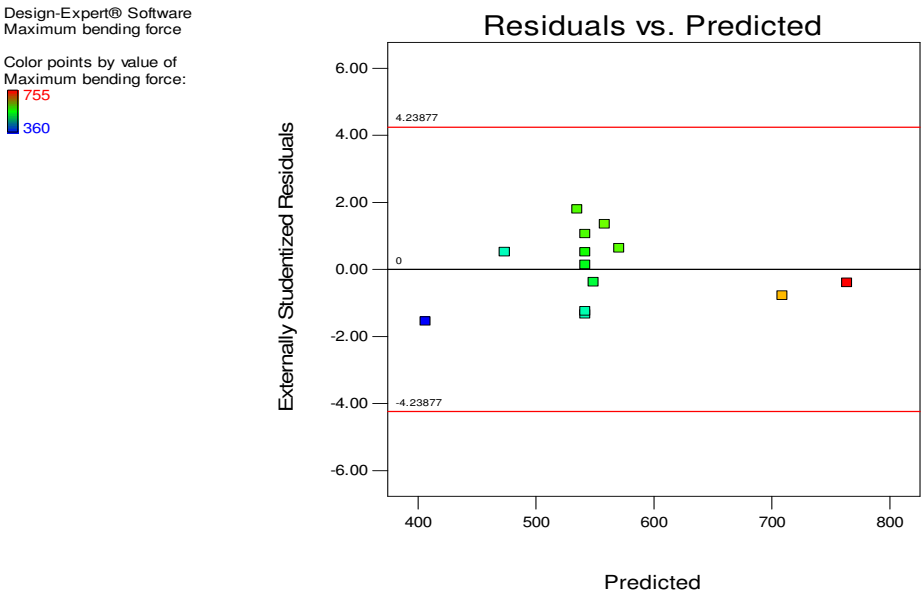

Fig. 9. Residual versus predicted data.

The predicted actual maximum bending force data against the actual ones for comparison reason were is depicted in figure (10). Figure (11) manifests the perturbation of maximum bending force, which shows the effect of both gas pressure and current on the maximum bending force over the range of the used levels. It was noted that the gas pressure has a greater impact on the maximum bending force than the current which is coded in term (A). However, figure (12) shows the combined influence of the two factors that occur after the central value (at nearly 95 Ampere current).

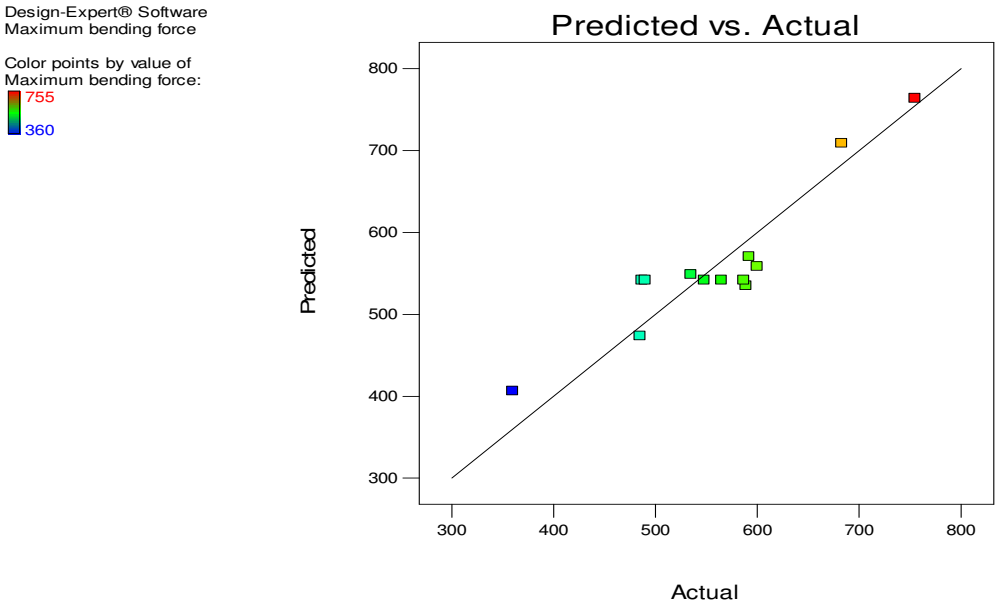

Fig. 10. Predicted versus actual data.

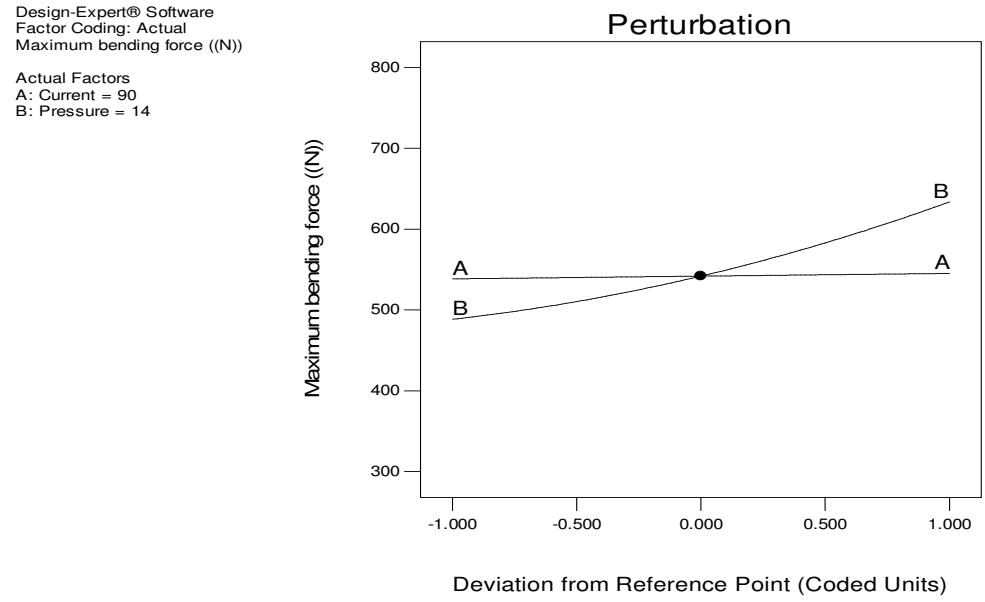

Fig. 11. Perturbation of maximum bending force.

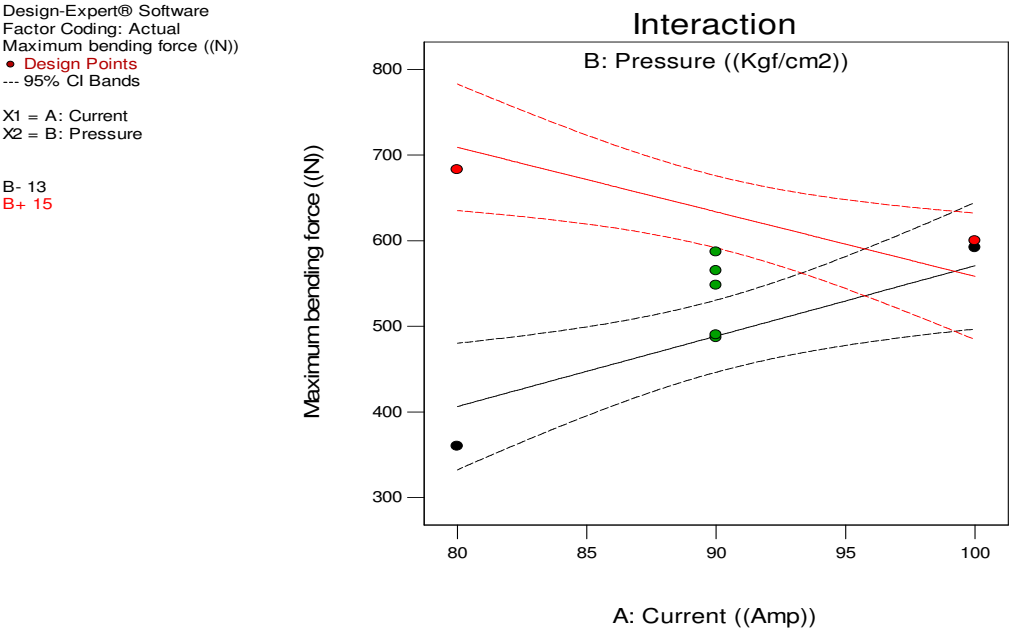

Fig. 12. Interaction of the gas pressure with the current.

Figure (13) illustrates the 2D contour graph of maximum bending force as a function of gas pressure and current. From this figure, it can be seen that the increase in gas pressure and current caused an increase in the maximum bending force. It can be noted that the increase of gas pressure value at the case of lower current (80 Amperes) leads to a maximum bending force of more than (665 N) because the more safeguard of the weld joint caused by the effect of higher gas pressure. While the increase of the current value (100 Amperes) at minimum value of gas pressure (13 Kgf/cm^2) resulted in more than (560 N) maximum bending force because the higher thermal impact resulted due to the higher quantity of heat input at the maximum current value. From the results above, both gas pressure and current have an influence on the maximum bending force, and the gas pressure has a greater effect on the bending force than the current value when analyzing these factors each one individually. Also, regarding the interaction of both factors gas pressure and weld current, also figure (13) shows that at nearly (95 Amperes and 14 Kgf/cm^2). The combined impact of the two factors gives a lower maximum bending force of about 535 N than that caused by each one individually.

The surface plot was explained in the 3D graph as viewed in figure (14) of maximum bending force as a function of current and gas pressure factors, and it confirms the perception mentioned above in the 2D graph. The increase of both factors current and gas pressure resulted in an increase in the maximum bending force value at their maximum level, while the gas pressure slightly higher, whereas at near their center level, i.e. at its higher level resulted in the maximum value of bending force at a higher level of current. Whereas, the lower level of both current and gas pressure caused the minimum value of max. bending force due to the less thermal effects.

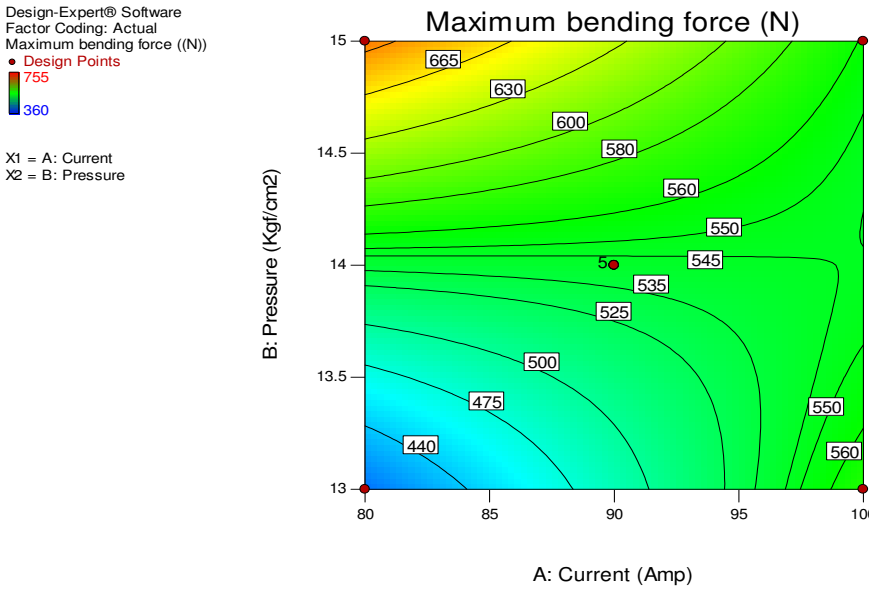

Fig. 13. 2D plot of maximum bending force as a function of current and gas pressure.

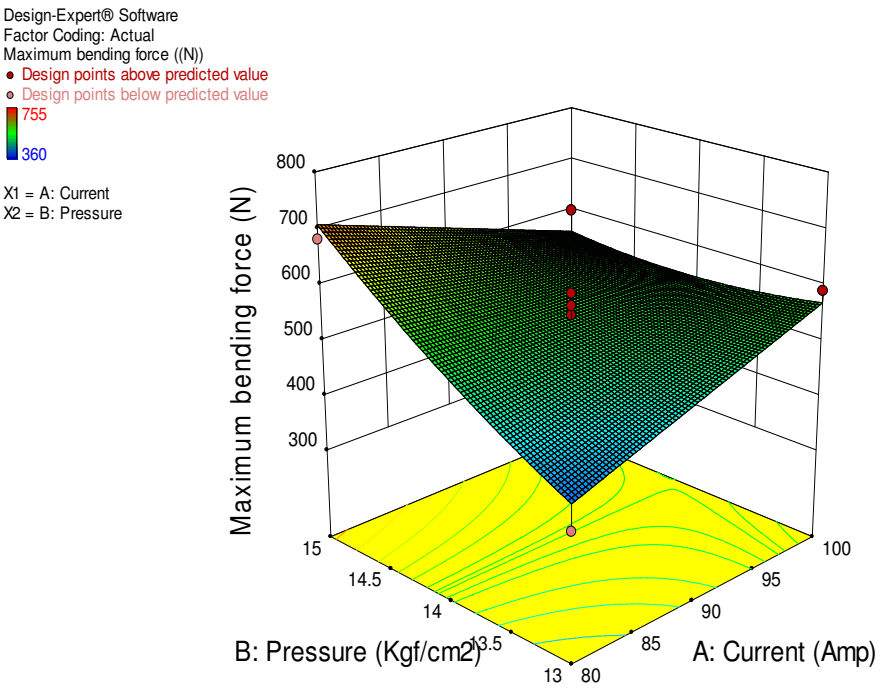

Fig. 14. 3D plot of maximum bending force as a function of current and gas pressure.

3.3 Optimization of the Maximum Bending Force

The DOE numerical optimization software was employed to obtain the optimum values of parameters in order to achieve the desired requirements of the welding joint, depending on the outcomes from the predicted quadratic models for the maximum bending force as responses as a function of two input factors (current and gas pressure). Table (6) manifests the constrains of optimization parameters and the goal of the output requirements.

Table 6,
Constrains of optimization

Name	Goal	Lower Limit	Upper Limit	Lower Weight	Upper Weight	Importance
Current (Amp)	is in range	80	100	1	1	3
Pressure (Kgf/cm^2)	is in range	13	15	1	1	3
Maximum bending force (N)	maximize	360	755	1	1	3

Desirability, which is a new objective function, was estimated and to be maximized through a numerical optimization to modify the predicted model, it ranges from 0 to 1 at the desired goal. The greater aim of this optimization was to determine the maximum result response that simultaneously met the variable maximum bending force. Constrain of the variable was used for numerical optimization of the maximum bending force, the input factors were selected for their used ranges, while the response was selected to be the maximum. Then according to this, it was found that one possible solution satisfied these constrains to determine the maximum values of the maximum bending force (709 N) as illustrates in table (7) with a maximum desirability value of (0.884) at the optimum values of weld current (80Amp) and gas pressure (15 Kgf/cm2).

Table 7,
The optimum values of input factors and outputs.

Current (Amp.)	Gas pressure (Kgf/cm^2)	Maximum bending force (N)	Desirability
80	15	709	0.884

3.4 Confirmation Tests at the Optimum Conditions

For more accuracy and to verify the validation of the maximum values of the maximum bending force shown in table (7), the confirmation tests were done at the optimum values of current and gas pressure. The confirmation tests average results are listed in table (8) for the comparison purpose between the results of experimental and predicted. The maximum error between the experimental and predicted for maximum bending force is about 3.8%. Figure (١٥) and figure (١٦) display the position of the maximum bending force in the 2D contour graph and 3D plot of optimum maximum bending force as a function of gas pressure and current, respectively. From these figures, it can be seen that the optimum maximum bending force resulted from the lower level of weld current (80 amperes) and the higher level of gas pressure (15 Kgf/cm^2).

Table 8,
Average results of confirmation tests at the optimum conditions

Current (Amp.)	Gas pressure (Kgf/cm^2)	Exp. Maximum bending force (N)	Pred. Maximum bending force (N)	Error (%)
80	15	683	709	3.8

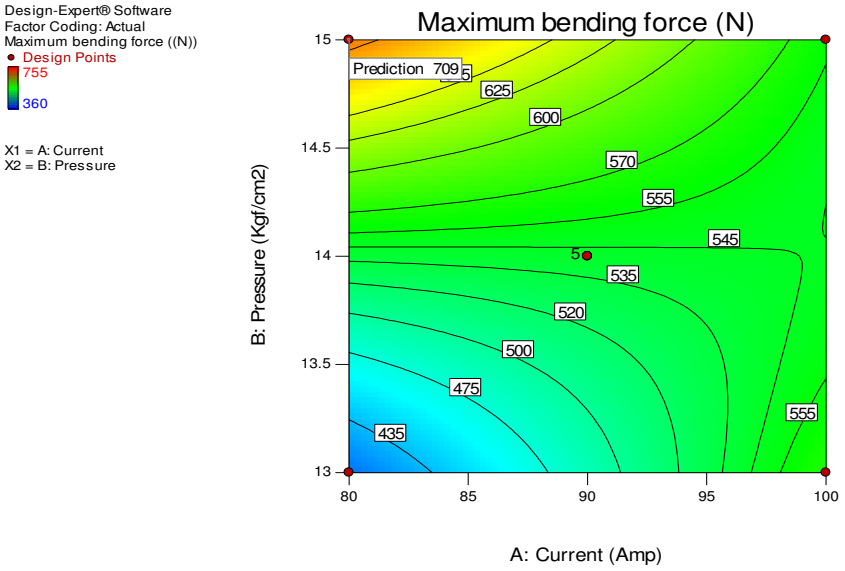

Fig. 15. 2D plot showing the position of the optimum maximum bending force.

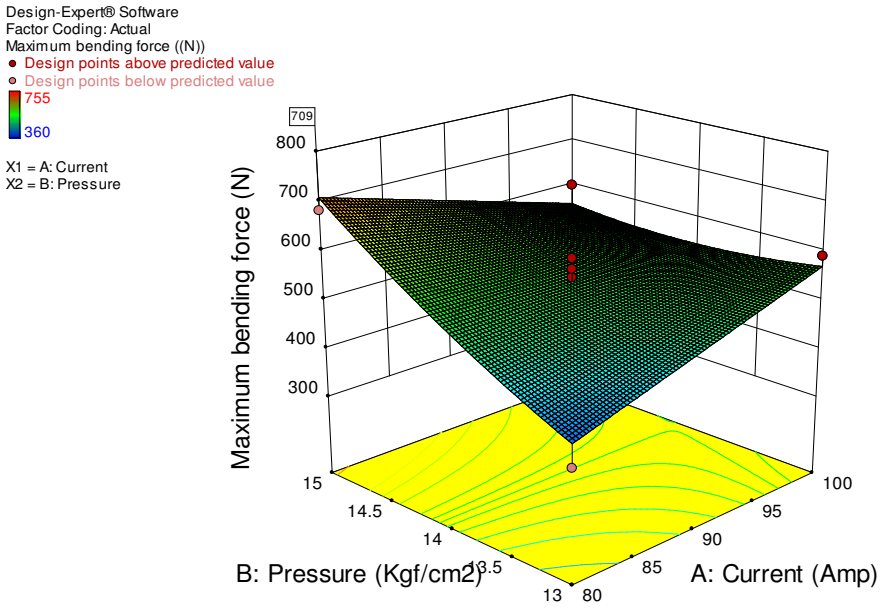

Fig. 16. 3D plot showing the position of the optimum maximum bending force.

4. Conclusions

The experimental and predicted results show that the increase in both gas pressure and current leads to an increase in the maximum bending force. However, the gas pressure has a greater impact on the maximum bending force than the current. According to the numerical optimization, the maximum value for the maximum bending force is (709 N) with a maximum desirability value of (0.884) at the optimum values of weld current (80 Amperes) and gas pressure (15 Kgf/cm^2). The confirmation tests prove that there is an agreement between the experimental and predicted results with a maximum error of (3.8%) for the maximum bending force. The increase of welding gas pressure increases the tensile strength, and the increase of both input factors (current and gas pressure) individually tends to a visual increase in the yield stress and elongation. Also, the combined effect of the input factors almost near their central level data gives the lowest values of the yield stress and elongation.

5. References

[1] V.A.Rao, and Dr. R. Deivanathan" experimental investigation for welding aspects of stainless steel 310 for the process of TIG welding", Elsevier Procedia Engineering, pp. 902 – 908, 2014.

[2] T.A.Tabish, T.Abbas, M.Farhan, S.Atiq, and T.Z.Butt, " Effect of heat input on microstructure and mechanical properties of the TIG welded joints of AISI 304 stainless steel ", International Journal of Scientific & Engineering Research, Vol .5, Issue 7, pp. 1532-1541, 2014.

[3] N. Moslemi, N. Redzuan, N. Ahmad, and T. Nan Hor, "Effect of current on characteristic for 316 stainless steel welded joint including microstructure and mechanical properties", Elsevier Procedia CIRP, pp.560 – 564, 2015.

[4] H. Zuhailawati, M. A. Jamaluddin, A. A. Seman, and S. Ismail, "Welding investigation and prediction of tensile strength of 304 stainless steel sheet metal joint by response surface methodology ", Elsevier Procedia Chemistry, pp. 217-221, 2016.

[5] Vikarm, and P. Sharma," Influence of process parameters on mechanical property of stainless steel 430 plate by TIG and MIG welding", International Journal for Scientific Research & Development, Vol. 4, Issue 10, pp. 40- 45, 2016.

[6] I.J. Rohit, R. Ajithraj and M. Dev Anand, "Experimental analysis of TIG Welded 304 stainless steel using artificial intelligence tool", International Journal of Pure and Applied Mathematics, Vol. 116, No. 22, pp. 365-373, 2017.

[7] M. Ravichandran, A. Naveen Sait, and U. Vignesh, " Investigation on TIG welding parameters of 2205 duplex stainless steel", international journal of automotive and mechanical engineering, Vol. 14, Issue 3, pp. 4518-4530, September 2017.

[8] A. Sohail, Abdul Aziz, M. Imran, O. Junaid, and S. Ahmed," Effect of TIG welding parameters on the properties of 304L automated girth welded pipes using orbital welding machine", Journal of Material Science, Vol. 5, Issue 4, pp.136-143, 2017.

[9] M. Saha, and, S. S. Dhami, "Effect of TIG welding parameter of welded joint of stainless steel SS304 by TIG Welding "Trends in mechanical engineering & technology, Vol. 8, Issue 3, pp.18-27, 2018

[10] D. Goyal, and P. Agrawal," Optimization of welding parameters of TIG welding on welding strength using taguchi and ANOVA " international journal for research in applied science & engineering technology, Vol. 6, Issue 3, pp.1250-1255, 2018.

[11] A. Jadhav, and. K. S.Wasankar," Optimisation of process parameters of A-TIG welding for penetration and hardness of SS 304 stainless steel weld" International Research Journal of Engineering and Technology, Vol. 5, Issue 10, pp.230-324, 2018.

[12] A. Balaram Naik, A. Chennakesava Reddy, and V. Venugopal Reddy," An experimental investigation of process parameters of tungsten inert gas welding for improvement of mechanical properties on duplex stainless steel (2205) weldments using design of experiments" Journal of Mechanical Engineering Research and Developments, Vol. 41, No.1, pp.86-96, 2018.

[13] M. A. Bayrak, V. Onar, and A. Işıtan," The investigation of microstructure and mechanical properties of austenitic stainless steel joints obtained by different welding methods and different welding parameters" SETSCI Conference Indexing System,Turkey, Vol. 3, pp.324-327, 2018.

[14] ASTM, "Standard specification for heat-resisting chromium and chromium-nickel stainless steel plate, sheet, and Strip for Pressure Vessels", A240, 2006.

[15] ASTM, "Standard test methods for tension testing of metallic materials", E8/E8M – 09, 2006.

[16] ASTM, "Standard test method for guided bend test for ductility of welds", E190-92, 2006.

منـ ة خواص الا حناء لصفائح الصلب المقاوم للصدأ 304 الملحومة بعملية لحام التنكستن مع الغاز الخامل

علي حسين علوان
قسم الهندسة الميكانيكية/ الجامعة التكنولوجية
البريد الالكتروني: 20145@uotechnology.edu.iq

الخلاصة

في هذا البحث، تم دراسة تأثير كل من ضغط غاز الأركون والتيار على خواص الانحناء للوصلات الملحومة. باستخدام المديات الممكنة لضغوط وتيارات غاز اللحام ، تم استخدام لحام غاز التنغستن الخامل (TIG) للفولاذ المقاوم للصدأ (٣٠٤) لايجاد تأثيره على أقصى قوة انحناء للمفاصل الملحومة بلحام (TIG). تم استخدام برنامج تصميم التجارب (DOE)، الإصدار العاشر لتحديد مصفوفة تصميم التجارب بالاعتماد على المديات المستخدمة لعوامل الادخال وتم استخدام تقنية منهجية سطح الاستجابة (RSM) للحصول على نموذج رياضي تجريبي للاستجابة لقوة الانحناء القصوى بوصفها دالة لعوامل اللحام (التيار وضغط غاز الأركون) وتم أيضاً أستخدام تحليل التباين (ANOVA) للتحقق ـصائياً من ملائمة النموذج الناتج.